CHEMICAL ENGINEERING TRANSACTIONS
VOL. 43, 2015
A publication of AIDIC
The Italian Association of Chemical Engineering
Online at www.aidic.it/cet
Chief Editors: Sauro Pierucci, Jiří J. Klemeš

ISBN 978-88-95608-34-1; **ISSN** 2283-9216
DOI: 10.3303/CET1543366

Design of the Integrated Solid Oxide Fuel Cell and Molten Carbonate Fuel Cell System to Reduce Carbon Dioxide Emissions

Prathak Jienkulsawad[a], Dang Saebea[b], Yaneeporn Patcharavorachot[c], Amornchai Arpornwichanop*[a]

[a]Computational Process Control Research Unit, Department of Chemical Engineering, Faculty of Engineering, Chulalongkorn University, Bangkok 10330, Thailand
[b]Department of Chemical Engineering, Faculty of Engineering, Burapha University, Chonburi 20131, Thailand
[c]School of Chemical Engineering, Faculty of Engineering, King Mongkut's Institute of Technology Ladkrabang, Bangkok 10520, Thailand
Amornchai.a@chula.ac.th

In general, a solid oxide fuel cell (SOFC) based on an internal reforming operation cannot be run with complete fuel utilization; therefore, the remaining fuel needs to be effectively handled. Furthermore, the SOFC exhaust gas still contains carbon dioxide, which is the primary greenhouse gas, and searching for the way to utilize this carbon dioxide is important. A molten carbonate fuel cell (MCFC) appears to be a potential technology to mitigate the emissions of carbon dioxide. In this study, the performance of the integrated SOFC and MCFC system is analyzed. The SOFC is considered a main power generation and the MCFC is regarded as a carbon dioxide concentrator along with producing electricity as a by-product. Mathematical models of the SOFC and MCFC are based on one-dimensional mass balances taking into all various cell voltage losses under steady-state and isothermal conditions. Primary operating conditions of the integrated fuel cell system that affects the system efficiencies in terms of power generation and reduction in the carbon dioxide emission are discussed and its optimal operation is identified based on these criteria. Effect of carbon dioxide recirculation on the system is also studied. Various configurations of the integrated SOFC-MCFC system are proposed and compared to determine the suitable design of the integrated fuel cell system.

1. Introduction

Fuel Cells are regarded as alternative power generation device that can directly convert chemical energy in fuel into electrical energy with high efficiency and environmental friendliness, compared to a conventional combustion-based process (Chatrattanawet et al., 2014). In general, types of fuel cells are classified by their operating temperatures. Solid oxide fuel cell (SOFC) and molten carbonate fuel cell (MCFC) are the high-temperature fuel cells (HTFC) that are typically operated at temperature over 600 °C. At this operating condition, heat produced from the fuel cells can be used in fuel processing and heat generation systems (McPhail et al., 2011).

As a hydrogen deficiency in cell stack causes collapse in physical structure, SOFC is basically operated at moderate fuel utilization (Saebea et al., 2014). Under this operation, the anode exhaust gas is still valuable because of remaining fuels, such as hydrogen and carbon monoxide. These useful fuels can be directly used in MCFC for producing additional power (Pastorino et al., 2011). Moreover, MCFC needs carbon dioxide circulation in its system; this means the MCFC appears to be a potential technology to mitigate the emissions of carbon dioxide (Wee, 2014). Hence, the integrated system of SOFC and MCFC is not only potential solution for increasing fuel utilization and power, but also reduces the carbon dioxide emissions. Different configuration designs of the SOFC-MCFC integrated system are possible. In this study, performance of such the fuel cell

Please cite this article as: Jienkulsawad P., Saebea D., Patcharavorachot Y., Arpornwichanop A., 2015, Design of the integrated solid oxide fuel cell and molten carbonate fuel cell system to reduce carbon dioxide emissions, Chemical Engineering Transactions, 43, 2191-2196
DOI: 10.3303/CET1543366

integrated system with different designs is investigated and compared in terms of power generation and carbon dioxide emissions.

2. System configuration

A planar SOFC consists of Ni-YSZ as anode, YSZ as electrolyte and YSZ-LSM as cathode. For MCFC, Ni-alloy is used as anode, Li_2CO_3/Na_2CO_3 is used as electrolyte and NiO is used as cathode. In the fuel cell integrated system, SOFC acts as a main power generation and MCFC as a carbon dioxide concentrator along with producing electricity as a by-product. Reformate gas from the reforming process is fed into the SOFC in order to maximize the power generation. The remaining fuels from the SOFC are introduced to the MCFC. In this study, three different configurations of the integrated system, as shown in Figure 1, are analyzed and compared to determine the suitable system design in terms of power generation and carbon dioxide emission. For the first configuration (A)(Figure 1(a)), the product of the SOFC is directly fed to the MCFC and portion of the exhaust gas from an after-burner is recirculated to the MCFC. This configuration is aimed at operating MCFC under less fuel concentration because of less fuel content in product of SOFC. In the second design (B)(Figure 1(b)), the reformate gas is separately fed to SOFC and MCFC. The anode off-gas from SOFC and MCFC are mixed with remaining gas from the cathode of MCFC and burnt in the after-burner and portion of the exhausted gas is recirculated. Configuration (B) aims to study the effect of increasing in feed to MCFC and consequently reduce feed to SOFC for increasing the amount of fuel feed to operate MCFC. In the third system configuration (C)(Figure 1(c)), the reformed gas is separately fed to SOFC and MCFC. The remaining gas from SOFC are mixed and burnt in the after-burner. The product gas from after-burner is fed to the cathode of MCFC. The anode off-gas from MCFC is fully recirculated. In the third configuration, the aim is adding MCFC on the downstream of the existing SOFC system by dividing the feed of SOFC to operate MCFC.

3. Mathematical model

The reactions that take place in the reformer, SOFC and MCFC are shown in Table 1. In the reformer, only the steam reforming reaction and water-gas shift reaction are considered and assumed to be at equilibrium. In SOFC and MCFC, the electrochemical reactions occur to generate electricity. A complete combustion reaction is assumed at the after-burner. Modelling of the SOFC and MCFC is based on one-dimensional mass balance and electrochemical model under steady-state and isothermal conditions.

3.1 Mass balance

Mass balance of gaseous components at the anode and cathode of the SOFC and MCFC can be written as below:

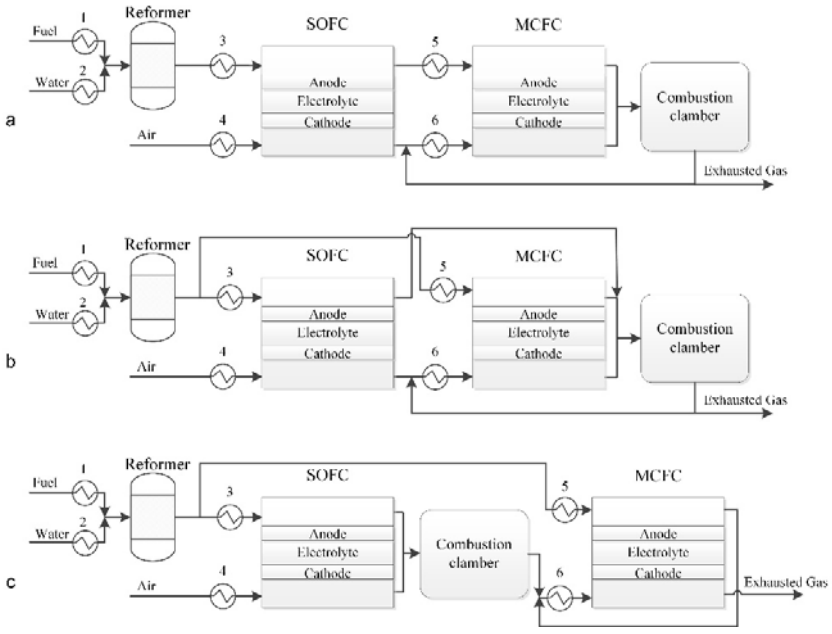

Figure 1: Configurations of the SOFC and MCFC integrated system

Table 1: List of reactions

Steam reforming	(i)	$CH_4 + H_2O \leftrightarrow 3H_2 + CO$
Water-gas shift	(ii)	$CO + H_2O \leftrightarrow H_2 + CO_2$
Hydrogen oxidation	(iii)	$H_2 + O^{2-} \rightarrow H_2O + 2e^-$
Oxygen reduction	(iv)	$0.5O_2 + 2e^- \rightarrow O^{2-}$
Overall cell (SOFC)	(v)	$H_{2,a} + 0.5O_{2,c} \rightarrow H_2O_{,a}$
Hydrogen oxidation	(vi)	$H_2 + CO_3^{2-} \rightarrow H_2O + CO_2 + 2e^-$
Oxygen reduction	(vii)	$0.5O_2 + CO_2 + 2e^- \rightarrow CO_3^{2-}$
Overall cell (MCFC)	(viii)	$H_{2,a} + 0.5O_{2,c} + CO_{2,c} \rightarrow CO_{2,a} + H_2O_{,a}$

$$\frac{\partial F_i}{\partial x} = W\left(\sum_k \nu_{i,k} R_k\right) \tag{1}$$

where F is the molar flow rate (mol s^{-1}), W is the cell width (m), ν is the stoichiometric coefficient of component *i* in the reaction *k* and R_k is the rate of reaction (mol m^{-2} s^{-1}).
The rates of reactions (R_k) in the SOFC are expressed as Eqs(2)-(4) for the steam reforming, water-gas-shift and electrochemical reaction, respectively (Patcharavorachot et al., 2010).

$$R_{SR} = k_0 p_{CH_4} p_{H_2O}^{-1.25} \exp\left(-\frac{E_a}{\Re T}\right) \tag{2}$$

$$R_{WGS} = k_{WGSR}\tau_a\left(p_{CO}p_{H_2O} - \frac{p_{CO_2}p_{H_2}}{K_{eq}}\right) \tag{3}$$

$$R_E = \left(\frac{j}{2F}\right)_{SOFC} \tag{4}$$

where k_{WGSR} is the pre-exponential factor (mol m^{-3} Pa^{-2} s^{-1}) and K_{eq} is the equilibrium constant given by:

$$k_{WGSR} = 0.0171\exp\left(-\frac{103191}{\Re T}\right) \tag{5}$$

$$\begin{aligned} K_{eq} &= \exp\left(-0.2935Z^3 + 0.6351Z^2 + 4.1788Z + 0.3169\right) \\ Z &= \frac{1000}{T} - 1 \end{aligned} \tag{6}$$

For the MCFC, the rates of reactions can be shown as Eqs(7)-(9) for the steam reforming, water-gas-shift and electrochemical reaction, respectively.

$$R_{SR} = \exp\left[Arr_{SR}\left(\frac{1}{a_{SR,1}} - \frac{298.15}{T}\right)\right] \times \left(y_{CH_4}y_{H_2O} - \frac{y_{CO}y_{H_2}^3}{K_{SR}}\right) \times \frac{a_{SR,2}}{LW} \tag{7}$$

$$R_{WGS} = \exp\left[Arr_{WGS}\left(\frac{1}{a_{WGS,1}} - \frac{298.15}{T}\right)\right] \times \left(y_{CO}y_{H_2O} - \frac{y_{CO_2}y_{H_2}}{K_{WGS}}\right) \times \frac{a_{WGS,2}}{LW} \tag{8}$$

$$R_E = \left(\frac{j}{2F}\right)_{MCFC} \tag{9}$$

Ovrum and Dimopoulos (2012) proposed the respective equilibrium coefficients (K_{SR} and K_{WGS}) and the values of the numerical constants (Arr_{SR}, Arr_{WGS}, $a_{SR,1}$, $a_{SR,2}$, $a_{WGS,1}$, $a_{WGS,2}$).

3.2 SOFC electrochemical model

The open-circuit voltage (E_{OCV}) of the SOFC is determined by Nernst equation:

$$E_{OCV} = E^0 - \frac{RT}{2F}\ln\left(\frac{p_{\mathrm{H_2O}}}{p_{\mathrm{H_2}}\, p_{\mathrm{O_2}}^{0.5}}\right) \tag{10}$$

where E^0 is the open-circuit voltage at standard pressure and it depends on temperature as shown in Eq(11)

$$E^0 = 1.253 - 2.4516e^{-4}T \tag{11}$$

However, there are internal losses inside the SOFC stack that make the actual voltage lower than the open-circuit called operating voltage (*E*) as (Aguiar et al., 2004):

$$E = E_{OCV} - \sum \eta_{loss} \tag{12}$$

The concentration overpotentials (η_{conc}) can be expressed as:

$$\eta_{\mathrm{conc,anode}} = \frac{RT}{2F}\ln\left(\frac{p_{\mathrm{H_2O},TPB}\, p_{\mathrm{H_2},f}}{p_{\mathrm{H_2O},f}\, p_{\mathrm{H_2},TPB}}\right) \tag{13}$$

$$\eta_{conc,\mathrm{cathode}} = \frac{RT}{4F}\ln\left(\frac{p_{\mathrm{O_2},a}}{p_{\mathrm{O_2},TPB}}\right) \tag{14}$$

The partial pressures (atm) at the three-phase boundaries (TPB) determined by using a gas transport model in porous material are shown in Eqs(15)-(17).

$$p_{\mathrm{H_2},TPB} = p_{\mathrm{H_2},f} - \frac{RT\tau_a}{2FD_{eff,a}}\, j \tag{15}$$

$$p_{\mathrm{H_2O},TPB} = p_{\mathrm{H_2O},f} + \frac{RT\tau_a}{2FD_{eff,a}}\, j \tag{16}$$

$$p_{\mathrm{O_2},TPB} = P - \left(P - p_{\mathrm{O_2},a}\right)\exp\left(\frac{RT\tau_c}{4FD_{eff,c}P}\, j\right) \tag{17}$$

The activation overpotentials (η_{act}) can be determined by the non-linear Butler-Volmer equation as follows:

$$j = j_{0,anode}\left[\frac{p_{\mathrm{H_2},TPB}}{p_{\mathrm{H_2},f}}\exp\left(\frac{\alpha nF}{RT}\eta_{act,\mathrm{anode}}\right) - \frac{p_{\mathrm{H_2O},TPB}}{p_{\mathrm{H_2O},f}}\exp\left(-\frac{(1-\alpha)nF}{RT}\eta_{act,\mathrm{anode}}\right)\right] \tag{18}$$

$$j = j_{0,\mathrm{cathode}}\left[\exp\left(\frac{\alpha nF}{RT}\eta_{act,\mathrm{cathode}}\right) - \exp\left(-\frac{(1-\alpha)nF}{RT}\eta_{act,\mathrm{cathode}}\right)\right] \tag{19}$$

where $j_{0,\mathrm{cathode}}$ and $j_{0,\mathrm{anode}}$ are the exchange current density (A m^{-2}) at the cathode and anode expressed as:

$$j_{0,\mathrm{anode}} = \frac{RT}{nF}k_{\mathrm{electrode}}\exp\left(-\frac{E_{\mathrm{electrode}}}{RT}\right) \tag{20}$$

$\mathrm{electrode} \in \{\mathrm{anode}, \mathrm{cathode}\}$

The ohmic losses (η_{ohm}) is as follows:

$$\eta_{ohm} = jR_{ohm} \tag{21}$$

where R_{ohm} is the internal resistance depending on the conductivity and the thickness of the individual layers as shown below:

$$R_{ohm} = \sum_i \frac{\tau_i}{\sigma_i} \tag{22}$$

where τ is the thickness (m), σ is the electronic conductivity (Ω^{-1} m^{-1}) and i represents the anode, cathode and electrolyte.

3.3 MCFC electrochemical model

The open-circuit voltage (E_{OCV}) of the MCFC is determined by Nernst equation:

$$E_{OCV} = -\frac{\Delta G}{2F} - \frac{RT}{2F}\ln\left(\frac{p_{H_2O}\, p_{CO_2,a}}{p_{H_2}\, p_{O_2}^{0.5}\, p_{CO_2,c}}\right) \tag{23}$$

where ΔG is the Gibbs free energy. The subscribe a and c mean the anode and cathode, respectively. The operating voltage (E) can be expressed as:

$$E = E_{OCV} - \sum \eta_{loss} \tag{24}$$

The internal voltage loss inside the MCFC based on a combined experimental and theoretical approach is defined as the equivalent global resistances which account for all type of losses. The equivalent global resistances are the resistances of the anode, cathode and electrolyte as follows (Morita et al., 2002):

$$R_{ir} = 1.12\times10^{-2}\exp\left(\frac{23}{RT}\right) \tag{25}$$

$$R_a = 2.04\times10^{-3}\exp\left(\frac{23.7}{RT}\right)p_{H_2}^{-0.5} \tag{26}$$

$$R_c = 3.28\times10^{-9}\exp\left(\frac{132}{RT}\right)p_{O_2}^{-0.75}\,p_{CO_2}^{0.5} + 3.39\times10^{-6}\exp\left(\frac{67.1}{RT}\right)y_{CO_2}^{-1} \tag{27}$$

where y_{CO_2} is the mole fraction of carbon dioxide at the cathode.

The total voltage losses can be written as Eq(28):

$$\sum \eta_{loss} = \left(R_{ir} + R_a + R_c\right) j \tag{28}$$

4. Results and discussion

Performance of the SOFC and MCFC integrated systems with different configurations is compared under the same operating condition. The performance is studied in term of the energy efficiency and the CO_2 emission coefficient that tell the amount of generated power per 1 kilogram of methane feed and the amount of CO_2 released to produce 1 kW-h electricity, respectively. The recycle ratio (R) is considered for the system configuration A and B. Increasing in recycle ratio increases the concentration of carbon dioxide in cathode of MCFC and consequently reduces the cathode resistance. In case of the system configuration B and C, the reformed gas is divided into two streams which identified by feed ratio (F). High feed ratio means that the large amount of the reformed gas is fed into the SOFC. Feed ratio told the proper fuel feed in each cell. High feed ratio may enhance the efficiency but the CO_2 may more release because of excess the CO_2 requirement in MCFC. Thus, the performance of the fuel cell systems varies, depending on the recycle ratio and the feed ratio. The simulation results show that for the configuration A, the energy efficiency increases with increasing the recycle ratio, but the CEC shows an opposite trend (Figure 2(a)). The fuel cell system A is preferred to be operated at a higher recycle ratio. For the system configuration B, the energy efficiency and the CEC rapidly increase when increasing in the feed ratio (Figure 2(b) and (c)). An increase in the recycle ratio also increases the energy efficiency, but decreases the CEC. At high feed ratio, the recycle ratio has a slight effect of the system performance. For the system configuration C (Figure 2(d)), increasing the feed ratio rises the energy efficiency of the fuel cell system. The CEC initially decreases to its minimum and then increases with the increased feed ratio. Figures 2(e) and (f) compare the energy efficiency and CEC of different fuel cell systems at their optimal operating conditions. It clearly shows that the system configuration A provides the highest energy efficiency and lowest CEC.

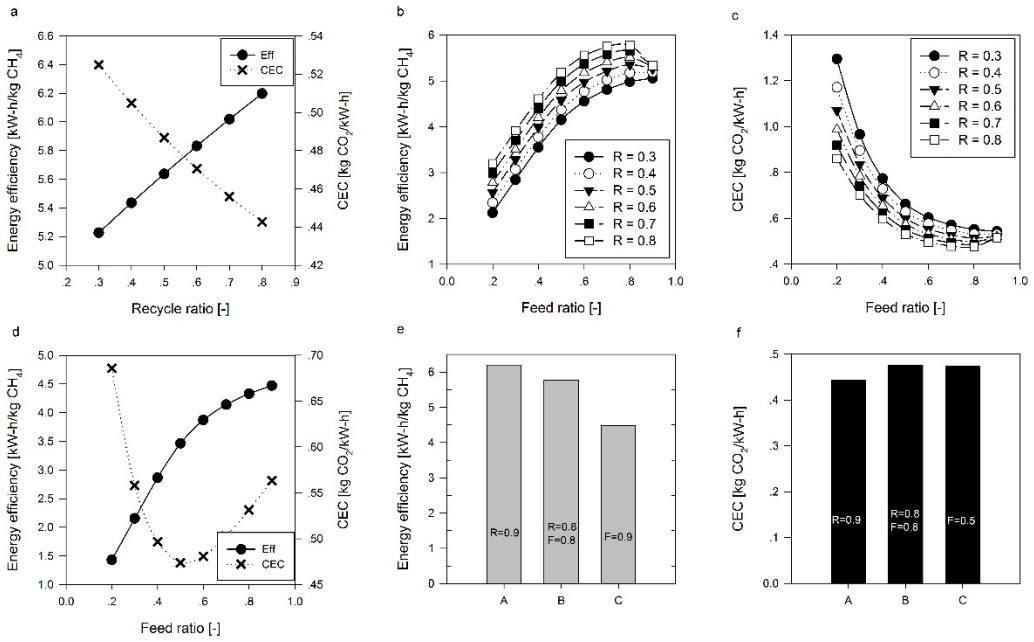

Figure 2: Performance of the fuel cell system: (a) Configuration A, (b) and (c) Configuration B and (d) Configuration C, and comparison of the system energy efficiency (e) and CEC (f)

5. Conclusions

This study investigated and compared the performance of the SOFC and MCFC integrated systems with different configurations in terms of power generation and CO_2 emission. The simulation results show that for the optimal fuel cell system, all the exhaust gases of the SOFC should be directly introduced to the MCFC and a recirculation of the exhaust gas from an after-burner to MCFC can enhance the energy efficiency and decrease the CO_2 emission.

Acknowledgements

Support from The Thailand Research Fund (The Royal Golden Jubilee Ph.D. Program and The Institutional Research Grant) and Chulalongkorn University is gratefully acknowledged.

References

Aguiar P., Adjiman C.S., Brandon N.P., 2004, Anode-supported intermediate temperature direct internal reforming solid oxide fuel cell. I: model-based steady-state performance, Journal of Power Sources, 138, 120-136.

Chatrattanawet N., Skogestad S., Arpornwichanop A., 2014, Control Structure Design and Controllability Analysis for Solid Oxide Fuel Cell, Chemical Engineering Transactions, 39, 1291-1296.

McPhail S.J., Aarva A., Devianto H., Bove R., Moreno A., 2011, SOFC and MCFC: Commonalities and opportunities for integrated research, International Journal of Hydrogen Energy, 36, 10337–10345.

Morita H., Komoda M., Mugikura Y., Izaki Y., Watanabe T., Masuda Y., Matsuyama T., 2002, Performance analysis of molten carbonate fuel cell using a Li/Na electrolyte, Journal of Power Sources, 112, 509–518

Ovrum E., Dimopoulos G., 2012, A validated dynamic model of the first marine molten carbonate fuel cell, Applied Thermal Engineering, 35 15-28.

Pastorino R., Budinis S., Currò F., Palazzi E., Fabiano B., 2011, Syngas Fuel Cells: Process Development to Risk Assessment, Chemical Engineering Transactions, 24, 1081-1086.

Patcharavorachot Y., Paengjuntuek W., Assabumrungrat S., Arpornwichanop A., 2010, Performance evaluation of combined solid oxide fuel cells with different electrolytes, International Journal of Hydrogen Energy, 35, 4301–4310.

Saebea D., Patcharavorachot Y., Arpornwichanop A., 2012, Analysis of an ethanol-fuelled solid oxide fuel cell system using partial anode exhaust gas recirculation, Journal of Power Sources, 208, 120–130.

Wee J.H., 2014, Carbon dioxide emission reduction using molten carbonate fuel cell systems, Renewable and Sustainable Energy Reviews, 32, 178-191.